

Symmetrical Angle Switched Single-Phase and Three-Phase Rectifiers: Application to Micro Hydro Power Plants

H. Bory*, L. Vazquez*, H. Martínez**, Y. Majanne***

*Electrical Engineering Faculty, University of Oriente, Ave. Las Americas s/n, 90400 Santiago of Cuba, Cuba (e-mail: bory@uo.edu.cu, lvazquez@uo.edu.cu, lvazquez0211@gmail.com)

** Departamento de Ingeniería Electrónica, Escuela de Ingeniería de Barcelona Este (EEBE), Universidad Politécnica de Cataluña (UPC) – BarcelonaTech, Av. De Eduard Maristany, n° 10 – 14, E-08019, Barcelona, España (e-mail: herminio.garcia@upc.es)

*** Lab. of Automation and Hydraulics, Tampere University of Technology, P.O. Box 692, FI-33101 Tampere, Finland (e-mail: yrjo.majanne@tut.fi)

Abstract: Micro-size hydro power plants are commonly used at remote areas to supply islanded AC micro-grids. A typical way to control grid frequency is to manipulate active power dissipated in ballast loads by AC/AC converters. However, these asymmetrically switched thyristor controlled converters consume reactive power degrading the power factor at the generator output. In this paper the operation of a symmetric angle switched, bridged three-phase rectifier and three single-phase rectifiers connected in series with ballast load, are studied to improve the power factor of the system. As a consequence, the objective is to evaluate the use of the three and single-phase rectifiers switched with symmetrical angle to improve the power factor, by reactive power compensation, at the output terminal of the electric generator of μ HPPs that use ballast load to regulate frequency.

Keywords: controlled rectifiers, switching AC/AC converters, power factor, symmetrical switching

1. INTRODUCTION

Due to climate issues and exhaustible resources of fossil energy, more and more attention has been paid to the utilization of renewable energy sources (López *et al.*, 2014; Wu *et al.*, 2014; Bordons *et al.*, 2015; García *et al.*, 2016; Castro *et al.*, 2016; Real *et al.*, 2017; Castro *et al.*, 2018 and Hohmeyer and Welle 2018). Distributed renewable generation based micro grids operated in island mode has become more popular to build energy self-sufficient areas, e.g. electrification of rural areas apart from national grids (Naqui *et al.*, 2013; Colak *et al.*, 2015; Farfán *et al.*, 2015; Farhat *et al.*, 2015; Ortega *et al.*, 2016 and Piris-Botalla *et al.*, 2016).

In Cuba, micro hydro power plants (μ HPPs) supplied micro grids are utilized in the electrification of off-grid rural areas. At this moment there are 117 μ HPPs placed mainly in provinces of the Orient region operating in island mode isolated from the National Electrical System. μ HPPs do not require big volumetric water flows, and they produce less harmful environmental impacts compared e.g. diesel generators. (Garcia, 2005; Renewable.cu, 2014 and Fong *et al.*, 2018)

Frequency regulation in μ HPP supplied islanded micro grids is typically done by manipulating the dissipated power in ballast loads controlled by AC/AC converters shunted with grid loads. The active power supplied by the generator (P_G) must equal with the dissipated power by the ballast load (P_L) plus the active power consumed by the users (P_U), Figure 1. The basic equation describing this type of regulation is: $P_G = P_L + P_U$

(Mare and Odello, 2001; Hechavarria and Bell, 2008; Peña *et al.*, 2013; Kurtz and Botteró, 2014; Vasquez *et al.*, 2014).

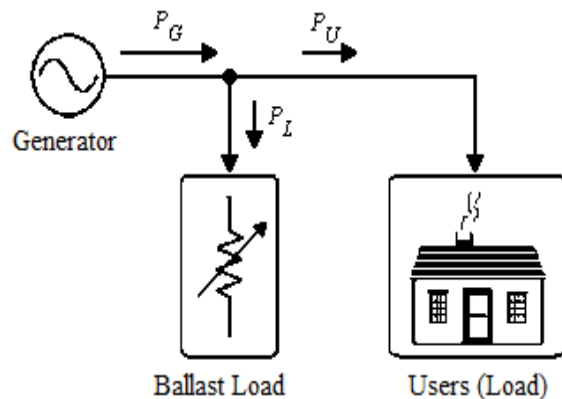


Figure 1. General scheme of the frequency regulation of a micro grid by the ballast load. (Hechavarria and Bell)

Kurtz and Botteró (2014) have shown that AC/AC converters consume reactive power degrading the power factor at the generator output terminals. The objective of this paper is to evaluate the use of three-phase and single-phase symmetrical angle switched rectifiers to improve the power factor by reactive power compensation at the output terminal of the generator in the frequency control of μ HPP supplied micro grids.

The evaluated system parameters are the effective current, the active, reactive, and apparent powers, distortion power and the power factor.

The structure of this paper is as follows: Chapters 2 and 3 present briefly operation principles of three-phase and single-phase rectifiers switched with symmetrical angle. Chapter 4 presents the μ HPP model built with Psim[®] modelling tool, and the equations for reactive power to demonstrate reactive power consumption of AC/AC converter. Chapter 5 introduces the application of the symmetrical angle switched rectifiers and makes a comparison with respect to the power factor at the output terminals of the generator.

2. THREE-PHASE BRIDGE RECTIFIER WITH A SWITCH IN SERIES WITH THE BALLAST LOAD

This chapter introduces the simulation scheme of the three-phase rectifier shown in figure 2 and the mathematical expressions of the evaluated system parameters (Bory *et al.* 2018).

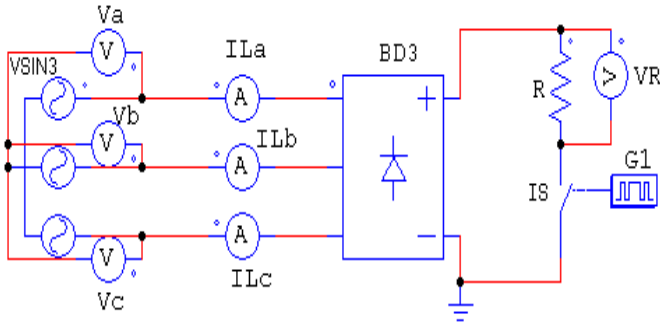


Figure 2. Simulation model of the three-phase rectifier and the switch-controlled ballast load implemented in Psim[®].

The simulation model consists of the following elements: three phase sinusoidal voltage source as a generator, (VSIN3), with frequency of 60 Hz and phase to phase effective voltage 190.53 V; a three phase diode bridge rectifier (BD3); an Isolated Gate Bipolar Transistor (IGBT) switch (IS); and the gating system (G1) producing the desired gating sequence to the switch. Parameters of the gating function are frequency (360 Hz), number of switching points (2), and switching point parameters (triggering angles and pulse width). The ballast load resistance is $R=4.03 \Omega$, and the measured voltages and currents are V_a , V_b , V_c , V_R , I_{La} , I_{Lb} and I_{Lc} . The measurements show the instantaneous wave forms of the voltage in each phase, the voltage across the ballast load R , and the phase currents in the rectifier input terminal.

Figure 3 shows the waveforms of voltages and currents of the rectifier circuit with a switching angle α of 15° .

The voltage-current phase angle φ_1 is zero for all switching angles. Thus, there are no phase shifts between the phase voltages and the first harmonics of the instantaneous currents in the input terminals of the rectifier.

The effective current at the rectifier input is:

$$I_{rms} = \frac{\sqrt{2}\sqrt{3}V_{ef}}{R} \sqrt{\frac{1}{\pi} \left[\frac{\pi}{3} - 2\alpha + \frac{\sqrt{3}}{2} \cos(2\alpha) - \frac{\sin(2\alpha)}{2} \right]} \quad (1)$$

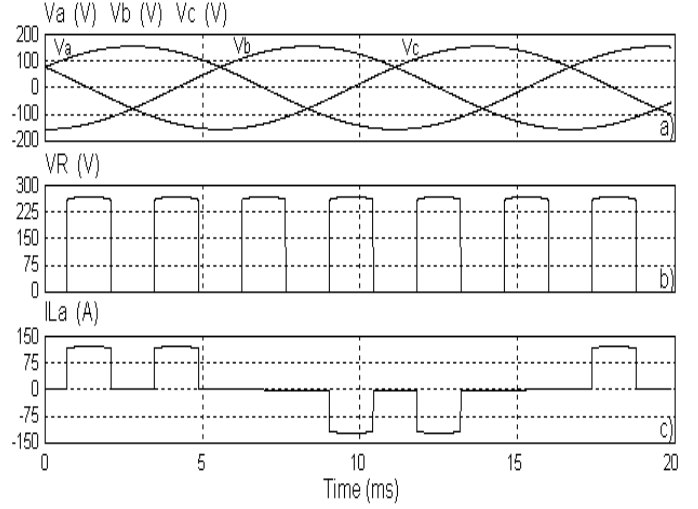


Figure 3. The wave forms of the three-phase rectifier switched with symmetrical angle. (a) Phase voltages at the generator output terminals, (b) Voltage across R , (c) Phase current I_{La} at the rectifier input terminal.

The active (P), reactive (Q), and apparent (S) powers and distortion power (T) at the rectifier input terminal are respectively:

$$P_{3ent} = \frac{9V_{ef}^2}{\pi R} \left[\frac{\pi}{3} - 2\alpha + \frac{\sqrt{3}}{2} \cos(2\alpha) - \frac{\sin(2\alpha)}{2} \right] \quad (2)$$

The maximum active power output is achieved with switching angle $\alpha = 0$.

$$Q_{3ent} = 0 \quad (3)$$

The result is evident for the zero voltage-current phase angle φ_1 , and it shows that the rectifier switched with symmetrical angle has no consumption of reactive power with any switching angle value.

$$S_{3ent} = \frac{3\sqrt{6}V_{ef}^2}{R} \sqrt{\frac{1}{\pi} \left[\frac{\pi}{3} - 2\alpha + \frac{\sqrt{3}}{2} \cos(2\alpha) - \frac{\sin(2\alpha)}{2} \right]} \quad (4)$$

The maximum apparent power output is achieved with switching angle $\alpha = 0$. The distortion power is

$$T_{3ent} = \frac{9V_{ef}^2}{\pi R} \sqrt{\frac{\pi^2}{9} - \left[2\alpha - \frac{\sqrt{3}}{2} \cos(2\alpha) + \frac{\sin(2\alpha)}{2} \right]^2} \quad (5)$$

For $\alpha = 0$, $T_{3ent} = 0.308P_{3entmax}$. This is different from zero, because the values of the currents at the rectifier input terminals are not sinusoidal. For $\alpha = \pi/6$, $T_{3ent} = 0$, because the current at the rectifier input terminals is zero.

The power factor of the rectifier is:

$$fp = \sqrt{\frac{3}{2\pi} \left[\frac{\pi}{3} - 2\alpha + \frac{\sqrt{3}}{2} \cos(2\alpha) - \frac{\sin(2\alpha)}{2} \right]} \quad (6)$$

Note, for $\alpha = 0$, the power factor $fp = 0.956$. As previously mentioned, for this angle the currents at the rectifier input terminals are not sinusoidal.

3. SINGLE-PHASE TYPE BRIDGE RECTIFIER WITH A SWITCH IN SERIES WITH THE BALLAST LOAD

In this chapter the simulation scheme of the single-phase rectifier with the symmetrically switch-controlled ballast load and the mathematical expressions of the system variables are presented. (Bory, Herminio, Vazquez, 2018).

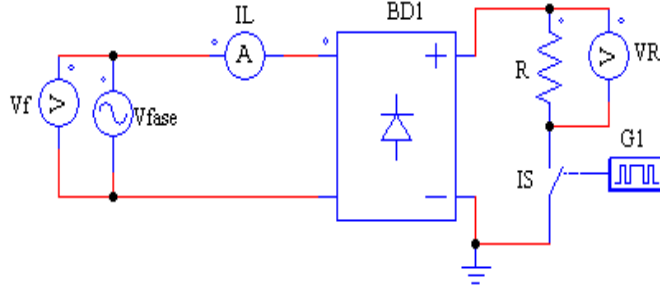


Figure 4. Simulation model of the single-phase rectifier and a switch-controlled ballast load implemented in Psim®.

The simulation model consists of the following elements: single phase sinusoidal voltage source (V_{fase}) with frequency 60 Hz and effective voltage 110 V; single phase diode bridge rectifier ($BD1$); Isolated Gate Bipolar Transistor ($IGBT$) switch (IS); and the gating system ($G1$) producing the desired gating sequence to the switch. Parameters of the gating function are frequency (120 Hz), number of switching points (2), and triggering angles and pulse widths of gating pulses. The ballast load resistance R is 4.03Ω , and the voltage and current measurements (V_f , V_R , I_L) show the instantaneous wave forms of the source voltage, the voltage across R and the current I_L at the rectifier input.

Figure 5 shows waveforms of the voltage and the current for the rectifier circuit with a switching angle of 30° .

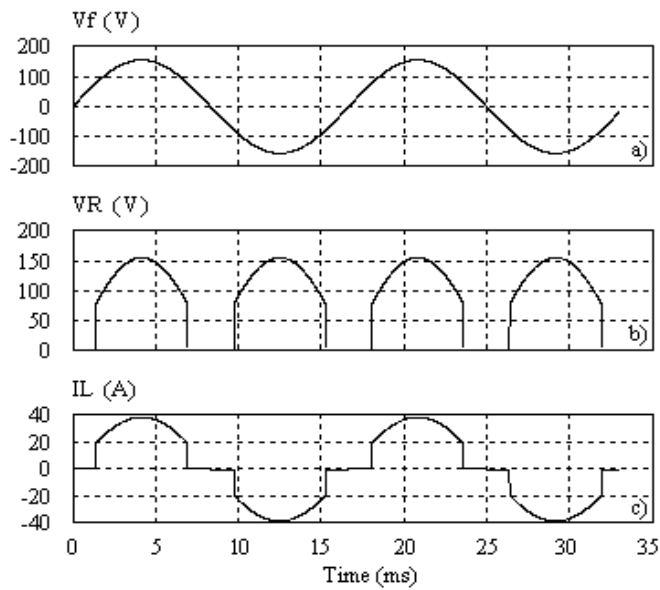


Figure 5. Wave forms of the single-phase rectifier switched with symmetrical angle. (a) Source voltage, (b) Voltage across R , (c) Current at the rectifier input terminal.

The voltage-current phase angle, ϕ_1 , is zero for all switching angle values, thus there is no phase shift between the phase voltage and the first harmonic of the instantaneous current to the rectifier input.

The effective current at the rectifier input is:

$$I_{rms} = \frac{V_{ef}}{R} \sqrt{\frac{\pi - 2\alpha + \sin(2\alpha)}{\pi}} \quad (7)$$

The active (P), reactive (Q), and apparent (S) powers, and the distortion power (T) at the rectifier input terminal are respectively:

$$P_{entBD} = \frac{V_{ef}^2}{\pi R} [\pi - 2\alpha + \sin(2\alpha)] \quad (8)$$

The maximum active power output is achieved with switching angle $\alpha = 0$.

$$Q_{3ent} = 0 \quad (9)$$

Again, this result is obtained from the mathematical expression of the voltage-current phase angle, and it informs that the rectifier switched with symmetrical angles does not consume reactive power at any switching angle value. The apparent power is

$$S_{entBD} = \frac{V_{ef}^2}{R} \sqrt{\frac{\pi - 2\alpha + \sin(2\alpha)}{\pi}} \quad (10)$$

The maximum apparent power $S_{entBDmax} = V_{ef}^2/R$ is achieved with $\alpha = 0$, and it equals with the maximum active power dissipated in the load resistance. Distortion power is

$$T_{entBD} = \frac{V_{ef}^2}{\pi R} \sqrt{[2\alpha - \sin(2\alpha)] \cdot [\pi - 2\alpha + \sin(2\alpha)]} \quad (11)$$

For $\alpha = 0$, $T_{entBD} = 0$. This is because with $\alpha = 0$, the current at the rectifier input terminal is sinusoidal. For $\alpha = \pi/2$ $T_{entBD} = 0$, because the current at the rectifier input terminal is zero.

The power factor to the input of the rectifier is

$$fp = \sqrt{\frac{\pi - 2\alpha + \sin(2\alpha)}{\pi}} \quad (12)$$

Note, for $\alpha = 0$, the power factor $fp = 1$. This is because the current at the rectifier input terminal is sinusoidal and there is no phase-shift between voltage and current.

4. PSIM MODEL FOR THE MICRO HYDROPOWER PLANT SCHEME

This chapter presents the Psim® model representing the μ HPP electric scheme. AC/AC converter is applied to regulate the power dissipated by the ballast load and to control the micro grid's system frequency. It is also shown that the AC/AC converter consumes inductive reactive power.

The system model presented in figure 6 consists of following components: sinusoidal voltage source $VSIN3$ (three-phase generator); grid load, $RLusers$; three AC/AC converters with gating units $G1$ to $G6$; ballast loads $Rballast 1$, $Rballast 2$ and $Rballast 3$; alternating current meters (ILa , ILb , ILc , $ILua$, $ILub$, $ILuc$, $IaBD$, $IbBD$, $IcBD$), Watt-meters, Var-meters,

VA and power factor meters (*W3L*, *VAR3L*, *VAPF3L*, *W3u*, *VAR3u*, *VAPF3u*, *W3BD*, *VAR3BD*, and *VAPF3BD*).

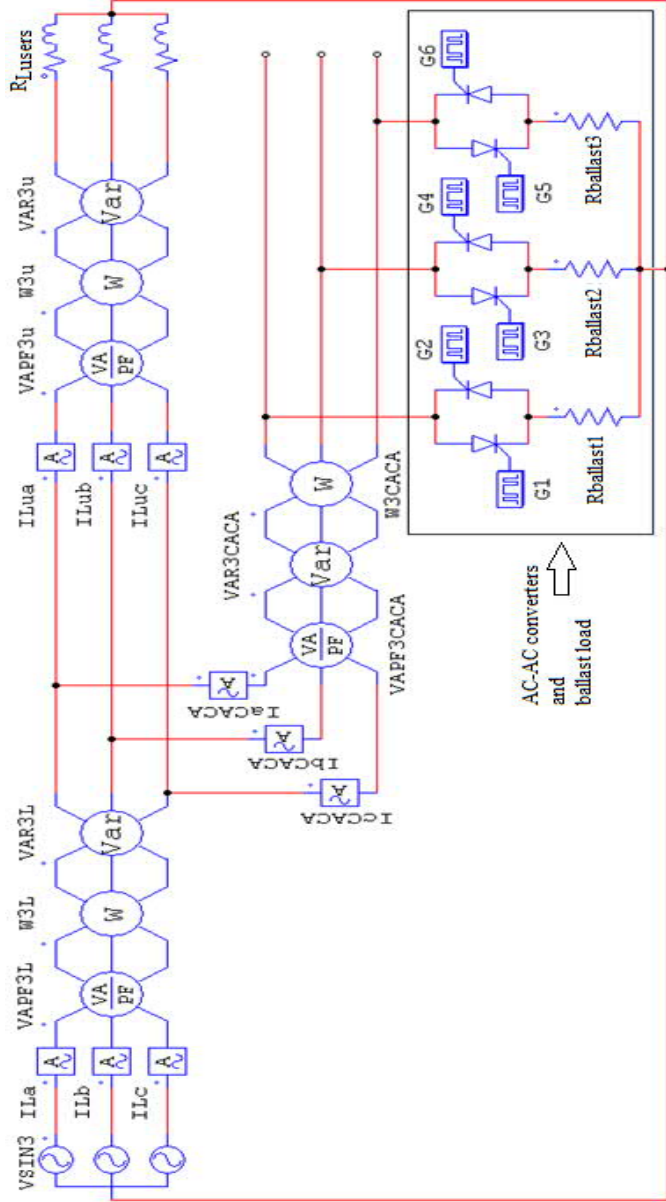


Figure 6. Simulation model (PSIM®) of the μ HPP generation-consumption system with three AC/AC converters controlling ballast loads. (Bory, 2011)

In (Bory, 2011 and Bory *et al.*, 2018), it has been demonstrated that the AC/AC converter has the disadvantage of consumption of inductive reactive power degrading the power factor at the generator output terminals. AC/AC converter's reactive power is

$$Q_{entAC/AC} = \frac{V_{ef}^2}{\pi R} \left[\frac{1 - \cos(2\alpha)}{2} \right] \quad (13)$$

Figure 7 shows the curve of the reactive power divided by the maximum active power as function of the triggering angle (α). The reactive power has its maximum value at $\alpha = \pi/2$ rad and it is 0.318 times the maximum active power.

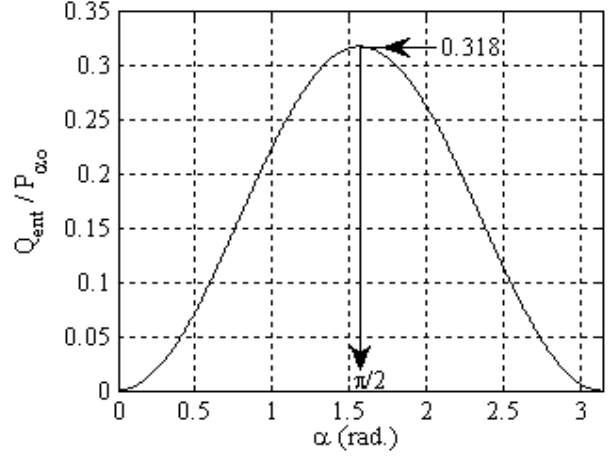


Figure 7: Q_{ent}/P_{ω_0} as a function of the triggering angle α (Bory, 2011; Bory *et al.*, 2018).

P_{ω_0} is the maximum active power at the AC/AC converter input, and it is obtained from the following expression with $\alpha = 0$.

$$P_{entAC/AC} = \frac{V_{ef}^2}{\pi R} \left[\pi - \alpha + \frac{\sin(2\alpha)}{2} \right] \quad (14)$$

5. APPLICATION OF THE SINGLE AND THREE-PHASE RECTIFIERS TO MICRO HYDROPOWER PLANTS

In this Chapter it is compared the symmetrically switched three-phase and single-phase rectifiers with Figure 6 type μ HPP scheme. The results show the power factor improvements at the electrical generator output terminals for load control schemes accomplished with symmetrical switched rectifiers.

The comparison is made with the following system: We have measurements from active power and effective current from the μ HPP. The minimum and maximum active power consumer loads are $P_{umin} = 3$ kW and $P_{umax} = 12$ kW. The users have an inductive power factor equal to 0.7.

The comparison is made by simulating the following schemes: Figure 6 type conventional AC/AC converter; the scheme replacing the conventionally controlled AC/AC converters with the three-phase rectifier switched with symmetrical angle.

Figure 8 represents the power factor at the generator output for the symmetrically switched three-phase rectifier, fp_{GsBD3} , and for the conventionally controlled AC/AC converters, fp_{GsACAC} .

Figure 8 shows that fp_{GsBD3} is bigger than fp_{GsACAC} only at the 94.5 % of the active power range P_U . Near to P_{umin} , fp_{GsBD3} is smaller than fp_{GsACAC} , 0.02 as maximum. That is because for the symmetrically switched rectifier the distortion power is greater than distortion and the inductive reactive powers consumed by the three AC/AC converters. The maximum difference of fp_{GsBD3} and fp_{GsACAC} is equal to 0.06.

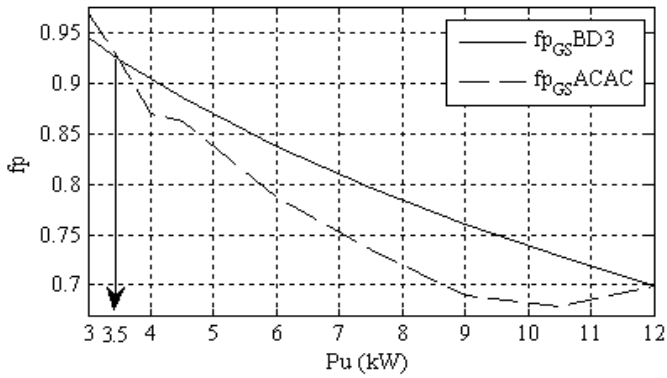


Figure 8. Comparison between the power factors at the generator output for the three-phase rectifier, fp_{GsBD3} , and the conventional AC/AC converters, fp_{GsACAC} .

Figure 8 shows that fp_{GsBD3} and fp_{GsACAC} have the same value, 0.94, for $P_U = 3.5$ kW.

The result indicates that it is possible to utilize the three-phase rectifier switched with symmetrical angle to improve the power factor at the generator output.

In the next case the objective is to study if it is possible to improve the power factor with the single phase rectifiers at the generator output through the entire consumer power range. The conventional AC/AC converter scheme is compared with the scheme where each AC/AC converter is replaced with a single phase rectifier switched with symmetrical angle.

Figure 9 represents the power factor at the generator output when the grid frequency is controlled by the three single phase rectifiers, fp_{GsBD} , and by the conventional AC/AC converters, fp_{GsACAC} .

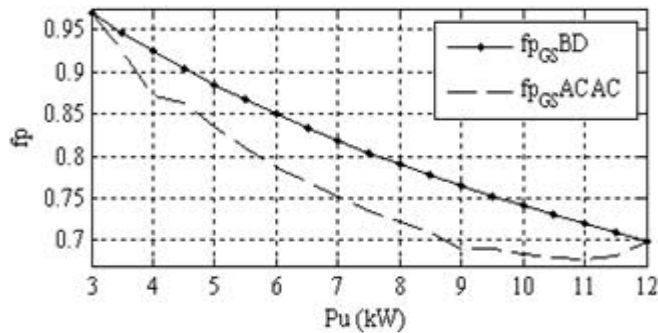


Figure 9. Comparison between the power factors at the generator output when the system is controlled by three single phase rectifiers, fp_{GsBD} , and by the conventional AC/AC converters, fp_{GsACAC} .

Figure 9 shows that fp_{GsBD} is bigger or equal than fp_{GsACAC} over the whole active power range P_U . At P_{Umin} , $fp_{GsBD} = fp_{GsACAC} = 0.97$, and at P_{Umax} for which $fp_{GsBD} = fp_{GsACAC} = 0.699$. The maximum difference between fp_{GsBD} and fp_{GsACAC} is equal to 0.075.

The simulation results show that in ballast load control the power factor at the generator output can be improved by substituting each AC/AC converter with a single phase rectifier switched with symmetrical angle.

ACKNOWLEDGEMENTS

This contribution is a result of EU's Erasmus+ programme financed CRECE project. The authors of the article gratefully acknowledge the financers and project partners.

REFERENCES

- Bordons, C., García-Torres, F., Valverde, L., (2015). Gestión Óptima de la Energía en Microrredes con Generación Renovable. Revista Iberoamericana de Automática e Informática industrial 12, 117–132. DOI: 10.1016/j.riai.2015.03.001
- Bory, H., (2011), Metodología para el mejoramiento del factor de potencia en Pequeñas Centrales Hidroeléctricas en régimen autónomo y que emplean convertidores de CA en CA para la regulación de frecuencia. Master Work. Automation Department. Electrical Engineering College. University of Oriente. Cuba.
- Bory, H., Martínez, H., Vázquez, L., Chang, F., Enríquez, L., (2018). Comparación entre Rectificador Trifásico con Conmutación Simétrica y Convertidor AC/AC para la Mejora del Factor de Potencia en Microcentrales Hidroeléctricas. Revista Iberoamericana de Automática e Informática industrial 15, 101–111. <https://doi.org/10.4995/riai.2017.8816>
- Bory, H., Martínez, H., Vázquez, L., (2018). Comparación entre Rectificador Monofásico con Conmutación Simétrica y Convertidor AC/AC para la Mejora del Factor de Potencia en Microcentrales Hidroeléctricas. Revista Iberoamericana de Automática e Informática industrial (accepted for publishing). <https://doi.org/10.4995/riai.2018.9313>
- Castro M. et al (2016), Integration of Renewable Energy Source in the Cuban Electric Power System, Project PR-759, Project Register System, Cujae, available at: http://www.cujae.edu.cu/investigaciones/sistema_de_registro_de_proyectos
- Castro M. et al (2018), Integration of Renewable Energy Sources in Cuba, Memories of Seminar Energy Future of Energy in Cuba, International Fair on Renewable Energy, Pabexpo, Havana, Cuba.
- Colak, I., Kabalci, E., Fulli, G., Lazarou, S., (2015). A survey on the contributions of power electronics to smart grid systems. Renewable Sustainable Energy 47, 562–579. doi:10.1016/j.rser.2015.03.031
- Farfán, R., Cadena, C., Villa, L., (2015). Experiencia en el uso de la Lógica Difusa para el Control del Seguimiento del Punto de Máxima Potencia en convertidores para Módulos Fotovoltaicos. Revista Iberoamericana de Automática e Informática industrial 12, 208–217. DOI: 10.1016/j.riai.2015.03.004
- Farhat, M., Barambones, O., Ramos, J., Duran, E., Andujar, J., (2015). Diseño e Implementación de un Sistema de Control estable basado en Lógica Borrosa para optimizar el rendimiento de un sistema de Generación Fotovoltaico. Revista Iberoamericana de Automática e Informática industrial 12, 476–487. DOI: 10.1016/j.riai.2015.07.006

- Fong J. et al. (2018). Design of a regulator of frequency, for small central hydroelectric in isolated operation. *Journal of Engineering and Technology for Industrial Applications*. DOI: <https://dx.doi.org/10.5935/2447-0228.20180021>.
- García, E., Correcher, A., Quiles, E., Morant, F., (2016). Recursos y sistemas energéticos renovables del entorno marino y sus requerimientos de control. *Revista Iberoamericana de Automática e Informática industrial* 13, 141–161. DOI: 10.1016/j.riai.2016.03.002
- Hechavarría, M., Bell, O., (2008). Control de frecuencia en centrales minihidroeléctricas aisladas, Graduated Final Work. Automation Department. Electrical Engineering College. University of Oriente, Cuba.
- Hohmeyer, O., Welle J. (2018) Cuban Society based on 100% renewable energy sources: A first scenario analysis. CRECEco-funded by the Erasmus + Programme of the European Union, Kick-Off January Weeks in Technological University of Havana and University of Oriente, Cuba.
- Kurtz, V., Botteró, F., Una alternativa para el control de cargas balasto que Regulan frecuencia y tensión en PCH de operación aislada. Available online: <http://www.cerpch.unifei.edu.br/arquivos/artigos/44c1e4324e3998d01c61875a2288b61.pdf>. Consulted: [19-05-2014].
- López, A., Somolinos, J., Núñez, L., (2014). Modelado Energético de Convertidores Primarios para el Aprovechamiento de las Energías Renovables Marinas. *Revista Iberoamericana de Automática e Informática industrial* 11, 224–235. DOI: 10.1016/j.riai.2014.02.005
- Mare, J., Odello, L., (2001). Reguladores de frecuencia inteligente para microcentrales hidráulicas. National University of COMAHUE, Argentina.
- Naqui, A., Ahmad, A., (2013). A lossless switching technique for smart grid applications. *Int J Electr Power Energy Syst* 49, 213 – 220.
- Ortega, R., Carranza, O., Sosa, J., García, V., Hernández, R., (2016). Diseño de controladores para inversores monofásicos operando en modo isla dentro de una microrred. *Revista Iberoamericana de Automática e Informática industrial* 13, 115–126. DOI: 10.1016/j.riai.2015.09.010
- Peña, L., Dominguez, H., Fong, J., Garcia, J., Alzórris, P., Regulación de frecuencia en una Minihidroeléctrica por carga lastre mediante un pc Embebido. Universidad Politécnica de Cataluña. Available online: <http://www.aedie.org/9CHLIE-paper-send/291-PE%D1A.pdf>. [Consulted: 12-06-2013]
- Piris-Botalla, L., Oggier, G., Airabella, A., García, G., (2016). Extensión del Rango de Operación con Conmutación Suave de un Convertidor CC-CC Bidireccional de Tres Puertos. *Revista Iberoamericana de Automática e Informática industrial* 13, 127–134. DOI: 10.1016/j.riai.2015.04.007
- Real, C., Moreno, A., Pallares, V., Gonzales, M., Moreno, I., Palacios, E., (2017). Sistema Electrónico Inteligente para el Control de la Interconexión entre Equipamiento de Generación Distribuida y la Red Eléctrica. *Revista Iberoamericana de Automática e Informática industrial* 14, 56–69. DOI: 10.1016/j.riai.2016.11.002
- Renovable.cu. Available online: http://www.google.com/cu/url?q=http://www.cubaenergia.cu/index.php/en/publications/doc_download/959-enero-2014&sa=U&ved=0CEUQFjAJahUKEwjlgae_0NPHAhVIaT4KHdCwADw&usq=AFQjCNHT_k03136THaOw3a0yaaUS hBsgBArenovable.cu. [Consulted: 12-01-2014]
- Vasquez, H., Pinedo, C., Palacios, J., Ramirez, J., Regulación de frecuencia en Micro-centrales hidroeléctricas mediante compensación de la carga. Universidad del Valle Available:<http://bibliotecadigital.univalle.edu.co/bitstream/10893/1216/1/Regulacion%20de%20frecuencia%20en%20microcenrales.pdf> [Consulted: 20-03-2014]
- Wu, D. et al (2014). Autonomous Active Power Control for Islanded AC Microgrids With Photovoltaic Generation and Energy Storage System. *IEEE Transactions on Energy Conversion* 4, 882-892.